A sparse Frequency-domain Bayesian filter for broadband source identification

Mathieu Aucejo

forum acusticum 2023

A SPARSE FREQUENCY-DOMAIN BAYESIAN FILTER FOR BROADBAND SOURCE IDENTIFICATION

Mathieu Aucejo[1*]
[1] Laboratoire de Mécanique des Structures et des Systèmes Couplés
Conservatoire National des Arts et Métiers, Hesam Université
Paris, France

ABSTRACT

In the frequency domain, broadband mechanical sources are typically identified frequency by frequency using Tikhonov-like regularization strategies. However, such an approach does not exploit the spectral characteristics of the sources to be identified, which can be detrimental to the quality of the identification, especially in the vicinity of the resonance frequencies of the structure. Based on this observation, mixed-norm regularization has been developed and applied with some success. However, this comes at the price of an increase in the computational cost, since the problem is solved for all frequencies at once. In order to reduce the computational cost of the identification procedure, while taking into account the spectral characteristics of the sources to identify, an original frequency-domain Bayesian filter is presented in this contribution. More precisely, the proposed strategy is a frequency-domain application of the Bayesian filtering theory to which Kalman filters belong. To evaluate the identification ability of the proposed approach, a numerical experiment is conducted on a simply-supported beam excited by a broadband point mechanical point force. A comparison with sparse regularization applied at each frequency independently is also proposed.

Keywords: *Bayesian filtering, Frequency domain, Inverse problem, Vibration*

**Corresponding author*: *mathieu.aucejo@lecnam.net.*

1. INTRODUCTION

Force reconstruction is a class of inverse problems aiming at estimating an excitation field applied on a mechanical structure from a set of vibration measurements. For solving such a problem in the frequency domain, several strategies have been implemented such as the virtual fields method [1] or the force analysis technique [2]. However, the most widely used technique is certainly the Tikhonov-like regularization which allows constraining the space of admissible solutions by incorporating some prior knowledge of the sources to identify. Among this class of methods, which derived from the Bayesian paradigm, one finds the ℓ_2-regularization (aka Tikhonov regularization) [3], ℓ_1-regularization [4], ℓ_p-regularization [5] or mixed-norm regularization [6].

Although these regularization strategies have proven their efficiency, some drawbacks remain when one wants to identify the space-frequency characteristics of broadband excitation sources. In this situation, ℓ_p-regularization ($p \in \mathbb{R}^{+*}$) generally solves the problem at each frequency separately. As a result, large reconstruction errors can be observed at the resonance frequencies (non-uniqueness of the solution). Furthermore, this resolution strategy ignores the fact that the excitation spectrum may have some continuity. While mixed-norm regularization overcomes this limitation to some extent, it is more computationally demanding as it solves the space-frequency problem all at once. Of course, by defining several non-overlapping frequency blocks, mixed-norm regularization can be run in parallel for each block. However, this requires a careful selection of the frequency bands.

To overcome the shortcomings mentioned above, it could be of great interest to approach the problem recursively, i.e. frequency by frequency while keeping track of the

spectrum continuity. In the time domain, Kalman filters are known to offer such a possibility with good reconstruction performances (see for example Ref. [7]). In this respect, the adaption of Kalman filtering in the frequency domain seems to be a promising approach. This strategy has already been successfully applied in the context of acoustic echo control by Enzner and Vary in Ref. [8].

With the previous idea in mind, the present contribution aims to introduce a novel Bayesian filter to identify broadband and spatially sparse excitation sources in the frequency domain. To this end, this paper is divided into three parts. The first section is dedicated to the description of the proposed frequency-domain Bayesian filter. More specifically, this section introduces the definition of the state-space representation of the identification problem, as well as the derivation of the Bayesian filter equations. In the second part, the filtering algorithm is presented, with a particular emphasis on the initialization step, which requires a special attention. Finally, a numerical experiment is implemented to evaluate the reconstruction ability of the proposed approach and to compare its performance with respect to ℓ_p regularization method.

2. FREQUENCY-DOMAIN BAYESIAN FILTER

This section presents the theoretical foundations of the proposed methodology. A special attention is paid on the derivation of the state-space model and the corresponding Bayesian filter.

2.1 State-space representation

Let us consider a linear and time invariant mechanical structure. In this situation, the noiseless vibration field $\mathbf{x}(\omega)$ is related to the excitation field $\mathbf{u}(\omega)$ by the transfer functions matrix $\mathbf{H}(\omega)$, which completely determines the dynamic behavior of the structure under consideration. This relation is given explicitly by:

$$\mathbf{x}(\omega) = \mathbf{H}(\omega)\,\mathbf{u}(\omega). \tag{1}$$

The state-space representation consists of a state equation, describing the evolution of the system state between two frequency steps, and an output equation relating the measured data to the system state and input.

The state equation is obtained by estimating the vibration field at a frequency $\omega + \delta\omega$, where $\delta\omega$ is a small frequency increment. By applying a first-order Taylor series, one has:

$$\mathbf{x}(\omega + \delta\omega) = \mathbf{x}(\omega) + \frac{\partial \mathbf{x}(\omega)}{\partial \omega}\delta\omega + \mathbf{w}(\omega), \tag{2}$$

where $\mathbf{w}(\omega)$ represents the modeling error related to unmodeled higher order terms. In the following, the modeling error is regarded as a process noise, which is supposed to be a complex Gaussian noise with zero mean and covariance matrix $\mathbf{Q}(\omega)$.

Then, the derivative of the vibration field w.r.t. ω can be approximated in the following way by using Eqn. (1) and applying first-order forward finite difference scheme:

$$\frac{\partial \mathbf{x}(\omega)}{\partial \omega}\delta\omega \approx \left[\mathbf{H}(\omega+\delta\omega) - 2\,\mathbf{H}(\omega)\right]\mathbf{u}(\omega) + \mathbf{H}(\omega)\mathbf{u}(\omega+\delta\omega). \tag{3}$$

Consequently, the state equation is given by:

$$\mathbf{x}_{k+1} = \mathbf{x}_k + \mathbf{B}_k^{-}\,\mathbf{u}_k + \mathbf{B}_{k+1}^{+}\mathbf{u}_{k+1} + \mathbf{w}_k, \tag{4}$$

where $\mathbf{x}_{k+1} = \mathbf{x}(\omega_k + \delta\omega)$ and $\mathbf{x}_k = \mathbf{x}(\omega_k)$. Here, $\mathbf{B}_k^{-} = \mathbf{H}_{k+1} - 2\,\mathbf{H}_k$ and $\mathbf{B}_{k+1}^{+} = \mathbf{H}_k$.

Regarding the output equation, it is obtained by assuming that the noiseless data are corrupted by an additive complex Gaussian noise $\mathbf{v}(\omega)$ with zero mean and covariance matrix $\mathbf{R}(\omega)$. It results that the output equation is such that:

$$\mathbf{y}_k = \mathbf{x}_k + \mathbf{v}_k, \tag{5}$$

where $\mathbf{y}_k$ is the measured vibration field at frequency ω_k.

Finally, the state-space representation is given by:

$$\begin{cases} \mathbf{x}_{k+1} = \mathbf{x}_k + \mathbf{B}_k^{-}\,\mathbf{u}_k + \mathbf{B}_{k+1}^{+}\mathbf{u}_{k+1} + \mathbf{w}_k \\ \mathbf{y}_k = \mathbf{x}_k + \mathbf{v}_k \end{cases}. \tag{6}$$

It should be noted that the previous formulation is non-standard, since the state vector at frequency step $k+1$ requires the knowledge of the input vector (i.e. excitation vector) at frequencies k and $k+1$. To reduce the state-space representation to its standard form, a reduced state $\overline{\mathbf{x}}_{k+1}$ is introduced. It is mathematically expressed as:

$$\overline{\mathbf{x}}_{k+1} = \mathbf{x}_k + \mathbf{B}_k^{-}\,\mathbf{u}_k + \mathbf{w}_k. \tag{7}$$

In doing so, the state-space representation becomes:

$$\begin{cases} \overline{\mathbf{x}}_{k+1} = \overline{\mathbf{x}}_k + \mathbf{B}_k\mathbf{u}_k + \mathbf{w}_k \\ \mathbf{y}_k = \overline{\mathbf{x}}_k + \mathbf{D}_k\,\mathbf{u}_k + \mathbf{v}_k \end{cases}, \tag{8}$$

where $\mathbf{B}_k = \mathbf{B}_k^{+} + \mathbf{B}_k^{-}$ and $\mathbf{D}_k = \mathbf{B}_k^{+}$.

2.2 Bayesian filter derivation

The present derivation is based on the unified sequential Bayesian formulation introduced by the author and his colleagues in Ref. [9]. It is briefly recalled for the sake of clarity and is divided into 6 steps:

0. Model definition – It is essentially a rewrite of Eqn. (8) from a Bayesian perspective:

$$\begin{aligned}\overline{\mathbf{x}}_{k+1} &\sim p(\overline{\mathbf{x}}_{k+1}|\overline{\mathbf{x}}_k, \mathbf{u}_k) = \mathcal{N}_c(\overline{\mathbf{x}}_{k+1}|\overline{\mathbf{x}}_k + \mathbf{B}_k\mathbf{u}_k, \mathbf{Q}_k)\\ \mathbf{y}_k &\sim p(\mathbf{y}_k|\overline{\mathbf{x}}_k, \mathbf{u}_k) = \mathcal{N}_c(\mathbf{y}_k|\overline{\mathbf{x}}_k + \mathbf{D}_k\mathbf{u}_k, \mathbf{R}_k),\end{aligned}$$

where $\mathcal{N}_c(\bullet|\mathbf{m}, \mathbf{\Gamma})$ is the complex Gaussian distribution with mean $\mathbf{m}$ and covariance matrix $\mathbf{\Gamma}$.

1. Initialization – This step requires the prior knowledge of the initial state and input vectors $\overline{\mathbf{x}}_0$ and $\mathbf{u}_0$, as well as the prediction of the state $\overline{\mathbf{x}}_1^*$ given the initial measurement $\mathbf{y}_0$. All these requirements are expressed as:

$$\begin{aligned}\overline{\mathbf{x}}_0 &\sim p(\overline{\mathbf{x}}_0) = \mathcal{N}_c(\overline{\mathbf{x}}_0|\widehat{\overline{\mathbf{x}}}_0, \mathbf{P}_0^{\overline{\mathbf{x}}})\\ \mathbf{u}_0 &\sim p(\mathbf{u}_0) = \mathcal{N}_c(\mathbf{u}_0|\widehat{\mathbf{u}}_0, \mathbf{P}_0^{\mathbf{u}}),\end{aligned}$$

where $\widehat{\overline{\mathbf{x}}}_0$ and $\widehat{\mathbf{u}}_0$ are the known mean state and input vectors, while $\mathbf{P}_0^{\overline{\mathbf{x}}}$ and $\mathbf{P}_0^{\mathbf{u}}$ are the related covariance matrices.

$$\begin{aligned}\overline{\mathbf{x}}_1 \sim p(\overline{\mathbf{x}}_1|\mathbf{y}_0) &= \iint_{\overline{\mathbf{x}}_0\,\mathbf{u}_0} p(\overline{\mathbf{x}}_1|\overline{\mathbf{x}}_0, \mathbf{u}_0)p(\overline{\mathbf{x}}_0)p(\mathbf{u}_0)d\overline{\mathbf{x}}_0 d\mathbf{u}_0\\ &= \mathcal{N}_c(\overline{\mathbf{x}}_1|\overline{\mathbf{x}}_1^*, \mathbf{P}_1^{\overline{\mathbf{x}}*}),\end{aligned}$$

where $\mathbf{P}_1^{\overline{\mathbf{x}}*}$ is the covariance matrix associated to the predicted mean state vector $\overline{\mathbf{x}}_1^*$.

2. Input prediction – This step requires the user to define the predictive distribution of the input vector given all the measurements collected up to the previous frequency step $k-1$, denoted $\mathbf{y}_{1:k-1} = \{\mathbf{y}_1, \ldots, \mathbf{y}_{k-1}\}$. Since our goal is to promote the spatial sparsity of the excitation field, the predictive distribution must reflect this behavior. In this contribution, it is chosen so that:

$$\mathbf{u}_k \sim p(\mathbf{u}_k|\mathbf{y}_{1:k-1}) = \prod_{i=1}^{N} \mathcal{N}_c(u_{ki}|0, \tau_{ki}^{-1}),$$

where u_{ki} is the i$^{\text{th}}$ component of the input vector at the frequency step k, while τ_{ki} is the corresponding precision parameter. N is the number of identification points.

Because each component of the input vector is considered has an independent normally-distributed complex random variable, the spatial sparsity is promoted by properly setting the value of the precision parameters (see Ref. [10]).

3. Input estimation – This step consists of applying the Bayes' rule to update our prediction of the input vector, given the information provided by the measurement at the current frequency step k. After some calculations, not detailed here, it comes:

$$\begin{aligned}\mathbf{u}_k \sim p(\mathbf{u}_k|\mathbf{y}_{1:k}) &\approx \int_{\overline{\mathbf{x}}_k} p(\mathbf{u}_k|\overline{\mathbf{x}}_k, \mathbf{y}_{1:k})p(\overline{\mathbf{x}}_k|\mathbf{y}_{1:k-1})d\overline{\mathbf{x}}_k\\ &= \mathcal{N}_c(\mathbf{u}_k|\widehat{\mathbf{u}}_k, \mathbf{P}_k^{\mathbf{u}}).\end{aligned}$$

4. State estimation – This step follows a similar procedure to that the input estimation. At this stage, it is also possible to compute the cross-covariance matrix $\mathbf{P}_k^{\overline{\mathbf{x}}\mathbf{u}}$. This results in:

$$\begin{aligned}\overline{\mathbf{x}}_k \sim p(\overline{\mathbf{x}}_k|\mathbf{y}_{1:k}) &= \int_{\mathbf{u}_k} p(\overline{\mathbf{x}}_k|\mathbf{u}_k, \mathbf{y}_{1:k})p(\mathbf{u}_k|\mathbf{y}_{1:k})d\mathbf{u}_k\\ &= \mathcal{N}_c(\overline{\mathbf{x}}_\mathbf{k}|\widehat{\overline{\mathbf{x}}}_k, \mathbf{P}_k^{\overline{\mathbf{x}}}),\end{aligned}$$

while, the cross-covariance matrix is given by:

$$\mathbf{P}_k^{\overline{\mathbf{x}}\mathbf{u}} = \iint_{\overline{\mathbf{x}}_k\,\mathbf{u}_k} (\overline{\mathbf{x}}_k - \widehat{\overline{\mathbf{x}}}_k)(\mathbf{u}_k - \widehat{\mathbf{u}}_k)^{\mathsf{H}} p(\overline{\mathbf{x}}_k, \mathbf{u}_k|\mathbf{y}_{1:k})d\overline{\mathbf{x}}_k d\mathbf{u}_k,$$

where $\mathbf{z}_k^{\mathsf{H}}$ is the Hermitian transpose of $\mathbf{z}_k$.

5. State prediction – This step consists of predicting the state vector at the next frequency step $k+1$ given the estimated state and input vectors at step k, i.e:

$$\begin{aligned}\overline{\mathbf{x}}_{k+1} &\sim p(\overline{\mathbf{x}}_{k+1}|\mathbf{y}_{1:k})\\ &= \iint_{\overline{\mathbf{x}}_k\,\mathbf{u}_k} p(\overline{\mathbf{x}}_{k+1}|\overline{\mathbf{x}}_k, \mathbf{u}_k)p(\overline{\mathbf{x}}_k, \mathbf{u}_k|\mathbf{y}_{1:k})d\overline{\mathbf{x}}_k d\mathbf{u}_k\\ &= \mathcal{N}_c(\overline{\mathbf{x}}_{k+1}|\overline{\mathbf{x}}_{k+1}^*, \mathbf{P}_{k+1}^{\overline{\mathbf{x}}*}).\end{aligned}$$

3. PRACTICAL IMPLEMENTATION

This section details the practical implementation of the Frequency-domain Bayesian filter introduced in the previous section.

3.1 General algorithm

Inputs – $\mathbf{y}_k$, $\widehat{\overline{\mathbf{x}}}_0$, $\mathbf{P}_0^{\overline{\mathbf{x}}}$, $\widehat{\mathbf{u}}_0$, $\mathbf{P}_0^{\mathbf{u}}$, $\mathbf{P}_0^{\overline{\mathbf{x}}\mathbf{u}}$, $\mathbf{B}_k$, $\mathbf{D}_k$, $\mathbf{Q}_k$, $\mathbf{R}_k$

Outputs – $\widehat{\mathbf{u}}_k$, $\mathbf{P}_k^{\mathbf{u}}$, $\widehat{\overline{\mathbf{x}}}_k$, $\mathbf{P}_k^{\overline{\mathbf{x}}}$

0. Initialization

$$\overline{\mathbf{x}}_1^* = \widehat{\overline{\mathbf{x}}}_0 + \mathbf{B}_0\,\widehat{\mathbf{u}}_0$$

$$\mathbf{P}_1^{\overline{\mathbf{x}}*} = \begin{bmatrix}\mathbf{I} & \mathbf{B}_0\end{bmatrix}\begin{bmatrix}\mathbf{P}_0^{\overline{\mathbf{x}}} & \mathbf{P}_0^{\overline{\mathbf{x}}\mathbf{u}} \\ \mathbf{P}_0^{\overline{\mathbf{x}}\mathbf{u}\mathsf{H}} & \mathbf{P}_0^{\mathbf{u}}\end{bmatrix}\begin{bmatrix}\mathbf{I} \\ \mathbf{B}_0^{\mathsf{H}}\end{bmatrix} + \mathbf{Q}_0$$

for *each frequency step* $k > 0$ **do**

1. Input estimation

$$\mathbf{i}_k = \mathbf{y}_k - \overline{\mathbf{x}}_k^*$$

$$\mathbf{P}_k^{\mathbf{u}*} = \mathbf{T}_k^{-1} \text{ with } \mathbf{T}_k = \text{diag}(\tau_{k1}, \ldots, \tau_{kN})$$

$$\mathbf{K}_k^{\mathbf{u}} = \mathbf{P}_k^{\mathbf{u}*}\mathbf{D}_k^{\mathsf{H}}(\mathbf{D}_k\mathbf{P}_k^{\mathbf{u}*}\mathbf{D}_k^{\mathsf{H}} + \mathbf{R}_k)^{-1}$$

$$\widehat{\mathbf{u}}_k = \mathbf{K}_k^{\mathbf{u}}\,\mathbf{i}_k$$

$$\mathbf{P}_k^{\mathbf{u}} = (\mathbf{I} - \mathbf{K}_k^{\mathbf{u}}\mathbf{D})\mathbf{P}_k^{\mathbf{u}*} + \mathbf{K}_k^{\mathbf{u}}\mathbf{P}_k^{\overline{\mathbf{x}}*}\mathbf{K}_k^{\mathbf{u}\mathsf{H}}$$

2. State estimation

$$\mathbf{K}_k^{\overline{\mathbf{x}}} = \mathbf{P}_k^{\overline{\mathbf{x}}*}(\mathbf{P}_k^{\overline{\mathbf{x}}*} + \mathbf{R}_k)^{-1}$$

$$\widehat{\overline{\mathbf{x}}}_k = \overline{\mathbf{x}}_k^* + \mathbf{K}_k^{\mathbf{x}}(\mathbf{i}_k - \mathbf{D}_k\widehat{\mathbf{u}}_k)$$

$$\mathbf{P}_k^{\overline{\mathbf{x}}} = (\mathbf{I} - \mathbf{K}_k^{\overline{\mathbf{x}}})\mathbf{P}_k^{\overline{\mathbf{x}}*} + \mathbf{K}_k^{\overline{\mathbf{x}}}\mathbf{D}_k\mathbf{P}_k^{\mathbf{u}}\mathbf{D}_k^{\mathsf{H}}\mathbf{K}_k^{\overline{\mathbf{x}}\mathsf{H}}$$

$$\mathbf{P}_k^{\overline{\mathbf{x}}\mathbf{u}} = -\mathbf{K}_k^{\overline{\mathbf{x}}}\mathbf{D}_k\mathbf{P}_k^{\mathbf{u}}$$

3. State prediction

$$\overline{\mathbf{x}}_{k+1}^* = \widehat{\overline{\mathbf{x}}}_k + \mathbf{B}_k\widehat{\mathbf{u}}_k$$

$$\mathbf{P}_{k+1}^{\overline{\mathbf{x}}*} = \begin{bmatrix}\mathbf{I} & \mathbf{B}_k\end{bmatrix}\begin{bmatrix}\mathbf{P}_k^{\overline{\mathbf{x}}} & \mathbf{P}_k^{\overline{\mathbf{x}}\mathbf{u}} \\ \mathbf{P}_k^{\overline{\mathbf{x}}\mathbf{u}\mathsf{H}} & \mathbf{P}_k^{\mathbf{u}}\end{bmatrix}\begin{bmatrix}\mathbf{I} \\ \mathbf{B}_k^{\mathsf{H}}\end{bmatrix} + \mathbf{Q}_k$$

end

3.2 Computation of the initial state and input distributions

In contrast to time domain applications, where it is possible to start the recordings with zero state and input vectors, a careful attention must be paid to the definition of the filter's starting conditions in the frequency domain.

Regarding the probability distribution of the initial state vector $\mathbf{x}_0$, a reasonable choice is:

$$\mathbf{x}_0 \sim \mathcal{N}_c(\mathbf{x}_0|\mathbf{y}_0, \mathbf{R}_0).$$

The probability distribution of the starting input vector $\mathbf{u}_0$ is supposed to be complex and Gaussian, with mean and covariance matrix derived from the following Bayesian regularization:

$$(\widehat{\mathbf{u}}_0, \widehat{\tau}_{0i}) = \underset{\mathbf{u}_0|\tau_{0i}}{\text{argmax}}\, p(\mathbf{y}_0|\mathbf{u}_0)\prod_{i=1}^{N} p(u_{0i}, \tau_{0i})\,p(\tau_{0i}). \quad (9)$$

In the previous equation:

$$p(\mathbf{y}_0|\mathbf{u}_0) = \mathcal{N}_c(\mathbf{y}_0|\mathbf{H}_0\mathbf{u}_0, \mathbf{R}_0)$$
$$p(u_{0i}|\tau_{0i}) = \mathcal{N}_c(u_{0i}|0, \tau_{0i}^{-1})$$
$$p(\tau_{0i}) = \mathcal{G}(\tau_{0i}|\alpha_i, \beta_i),$$

where $\mathcal{G}(\bullet|\alpha_{0i}, \beta_{0i})$ is the gamma distribution with shape parameter $\alpha_{0i} = 1$ and rate parameter $\beta_{0i} = 10^{-18}$.

After solving the optimization problem given by Eqn. (9) from an iterative procedure not described here, it comes that:

$$\widehat{\mathbf{u}}_0 = (\mathbf{H}_0\mathbf{R}_0^{-1}\mathbf{H}_0 + \widehat{\mathbf{T}}_0)^{-1}\mathbf{H}_0^{\mathsf{H}}\mathbf{R}_0^{-1}\mathbf{y}_0$$
$$\mathbf{P}_0^{\mathbf{u}} = (\mathbf{H}_0\mathbf{R}_0^{-1}\mathbf{H}_0 + \widehat{\mathbf{T}}_0)^{-1},$$

where $\widehat{\mathbf{T}}_0 = \text{diag}(\widehat{\tau}_{01}, \ldots, \widehat{\tau}_{0N})$.

To complete the initialization process, it remains to determine the parameters of the complex Gaussian distribution associated with the reduced state $\overline{\mathbf{x}}_0$. From Eqn. (4) and Eqn. (7) and assuming that $\mathbf{x}_0$ and $\mathbf{u}_0$ are uncorrelated, one has:

$$\widehat{\overline{\mathbf{x}}}_0 = \widehat{\mathbf{x}}_0 - \mathbf{B}_0^{+}\widehat{\mathbf{u}}_0$$
$$\mathbf{P}_0^{\overline{\mathbf{x}}} = \mathbf{R}_0 + \mathbf{B}_0^{+}\mathbf{P}_0^{\mathbf{u}}\mathbf{B}_0^{+\mathsf{H}}.$$

From what precedes, it is also possible to derive the expression of the initial cross-covariance matrix $\mathbf{P}_0^{\overline{\mathbf{x}}\mathbf{u}}$. After some calculations, one gets:

$$\mathbf{P}_0^{\overline{\mathbf{x}}\mathbf{u}} = -\mathbf{B}_0^{+}\mathbf{P}_0^{\mathbf{u}}.$$

3.3 Computation of the estimated input vector

At a frequency step k, it can be demonstrated that the estimated input vector $\widehat{\mathbf{u}}_k$ is solution of the following minimization problem (see Ref. [9] for details):

$$\widehat{\mathbf{u}}_k = \underset{\mathbf{u}_k}{\text{argmax}}\, p(\mathbf{i}_k|\mathbf{u}_k)\,p(\mathbf{u}_k), \quad (10)$$

where:

$$p(\mathbf{i}_k|\mathbf{u}_k) = \mathcal{N}_c(\mathbf{i}_k|\mathbf{D}_k\mathbf{u}_\mathbf{k}, \mathbf{R}_k)$$
$$p(\mathbf{u}_k) = \prod_{i=1}^{N}\mathcal{N}_c(u_{ki}|0, \tau_{ki}^{-1}).$$

Unfortunately, since it is far from easy to determine a priori suitable values for the precision parameters τ_{ki}, it may be interesting to consider them as random variables and

compute their values by optimization. To do this, one has to extend the previous optimization problem in such a way that:

$$(\widehat{\mathbf{u}}_k, \widehat{\tau}_{ki}) = \underset{\mathbf{u}_k, \tau_{ki}}{\operatorname{argmax}}\, p(\mathbf{i}_k|\mathbf{u}_k) \prod_{i=1}^{N} p(u_{ki}|\tau_{ki})\, p(\tau_{ki}), \quad (11)$$

where:

$$p(u_{ki}|\tau_{ki}) = \mathcal{N}_c(u_{ki}|0, \tau_{ki}^{-1})$$
$$p(\tau_{ki}) = \mathcal{G}(\tau_{ki}|\alpha_{ki}, \beta_{ki}),$$

with $\alpha_{ki} = 1$ and $\beta_{ki} = 10^{-18}$.

After convergence of an iterative procedure implemented to solve Eqn. (11), one obtains the estimated input vector $\widehat{\mathbf{u}}_k$ and the corresponding covariance matrix $\mathbf{P}_k^{\mathbf{u}}$ according the set of equations presented in step 1 of the algorithm described in section 3.1.

4. NUMERICAL EXPERIMENT

This section aims to validate the proposed Frequency-domain Bayesian filter (FBF) and compare its performance with sparse ℓ_p-regularization ($p \leq 1$) applied at each frequency separately.

4.1 Problem statement

The structure under consideration is a simply supported stainless steel beam. The beam is 1 m long, 3 cm wide and 1 cm thick. The material properties are $E = 210$ GPa for the Young's modulus and $\rho = 7850$ kg.m^{-3} for the density. A structural damping factor is assumed and set to 1%.

Along the beam, a set of 20 accelerometers are mounted on the structure and one of these sensors is collocated with the excitation at $x_0 = 63$ cm as presented in Fig. 1.

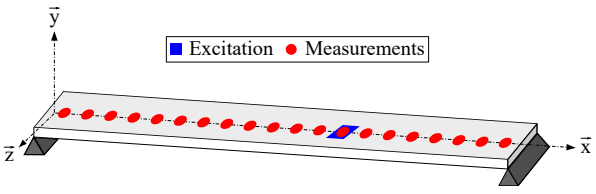

Figure 1: Definition of the numerical experiment

Regarding the excitation spectrum to identify, it is supposed that the structure is excited by a unit point force between 50 Hz and 1 kHz. The frequency resolution is set to 0.5 Hz. In this frequency range, the beam has 5 modes (94 Hz, 211 Hz, 375 Hz, 586 Hz and 844 Hz).

In the present experiment, the noiseless vibration data have been generated using a finite element model. Then, they have corrupted by an additive Gaussian white noise with a controlled signal-to-noise ratio set to 25 dB. On the other hand, the transfer functions matrices, required to construct the state-space representation, have been computed analytically from a classical mode expansion using the first 10 modes of the structure (i.e. up to 2.3 kHz).

To run the proposed filter, it remains to define the covariance matrices $\mathbf{Q}_k$ and $\mathbf{R}_k$. These matrices are assumed to be isotropic and constant, i.e. they are defined only by their variances σ_x^2 and σ_y^2 respectively.

Since the process noise reflects our confidence in the evolution model associated with the reduced state $\overline{\mathbf{x}}_k$, the value of σ_x^2 must be chosen accordingly. Given the frequency resolution chosen for this application, it is reasonable to assume that the evolution model is reliable. For this reason, σ_x^2 is set to 10^{-10}.

Regarding the measurement noise variance, its value is perfectly known, since the noise level is controlled. In practice, however, it has to be estimated either from calibration measurements or from a dedicated procedure. In this contribution, the measurement noise variance is estimated using a procedure inspired by Ref. [11]. This gives $\sigma_y^2 = 0.084$ m^2/s^4, which is close to the actual value of 0.083 m^2/s^4.

4.2 Application

In this contribution, the results obtained with FBF are compared to the ℓ_p-regularization solved at each frequency independently. Here, the value of p is set to 0.5 in order to promote the spatial sparsity of the excitation field. Formally, the latter regularization strategy is expressed as:

$$\widehat{\mathbf{u}}_k = \underset{\mathbf{u}_k}{\operatorname{argmin}} \|\mathbf{y}_k - \mathbf{H}_k\mathbf{u}_k\|_{\mathbf{R}_k}^2 + \lambda\|\mathbf{u}_k\|_p^p,$$

where λ is the regularization parameter and $\|\mathbf{x}\|_{\mathbf{R}}^2 = \mathbf{x}^{\mathsf{H}}\mathbf{R}^{-1}\mathbf{x}$.

From a practical point of view, ℓ_p-regularization is solved by an Iteratively Reweighted Least-Squares algorithm, which updates the regularization parameter at each iteration from the L-curve principle (see Ref. [5] for details).

Fig. 2 compares the space-frequency distribution of reconstructed excitation source from the FBF and ℓ_p-regularization. In particular, it can be seen that the FBF allows to obtain a source distribution closer to the real one than the ℓ_p-regularization, which shows large discrepancies at some resonance frequencies and artifacts.

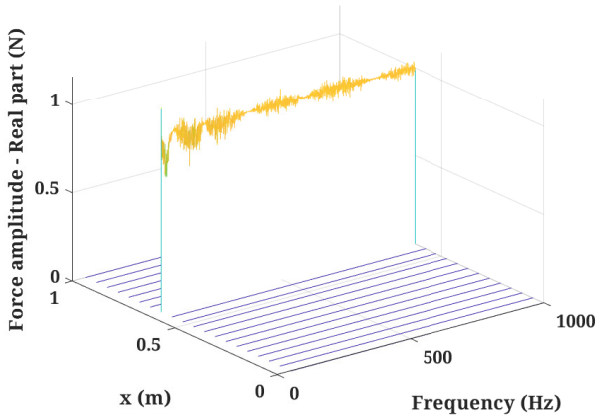

(a) Frequency-domain Bayesian Filter

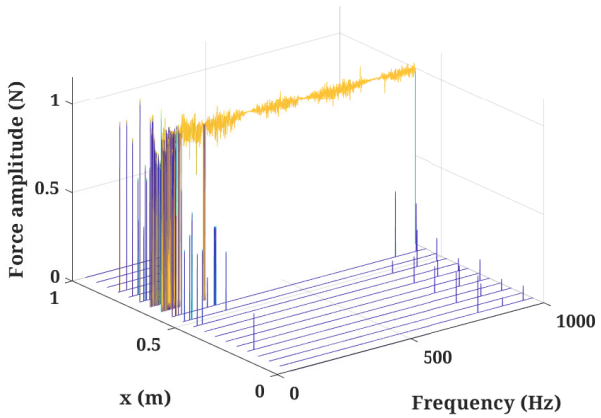

(b) ℓ_p-regularization ($p = 0.5$)

Figure 2: Comparison of the space-frequency distribution of the reconstructed excitation field

A closer look at the reconstructed force spectrum is proposed in Fig. 3. It confirms that the proposed FBF behaves better than the ℓ_p-regularization, especially around the resonance frequencies at 94 Hz and 211 Hz. To better quantify the reconstruction quality, we define the reconstruction error as:

$$RE = \frac{\|\widehat{u}_k - u_k^{\text{ref}}\|_1}{\|u_k^{\text{ref}}\|_1},$$

where $\widehat{u}_k$ is the identified force at the point force location, while u_k^{ref} is the reference value (here 1 N).

In the present application, $RE = 3.26\%$ for the FBF and $RE = 6.41\%$ for the ℓ_p-regularization, confirming what was visually inferred from the inspection of Fig. 3.

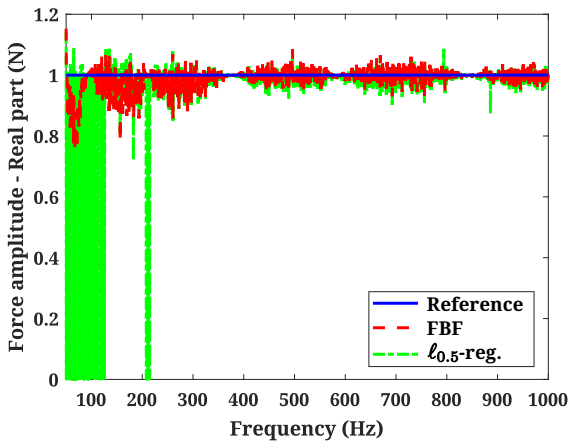

Figure 3: Comparison of the reconstructed force spectrum

5. CONCLUSION

This contribution has described a novel Frequency-domain Bayesian filter for the identification of broadband sparse excitation sources. The present Bayesian filter has a structure similar to the Kalman-like filters classically used for time-domain applications. The numerical experiment has demonstrated the potential benefits of the proposed strategy, as it allows to obtain consistent reconstructions even at resonance frequencies, where sparse regularization generally fails.

6. REFERENCES

[1] A. Berry, O. Robin, and F. Pierron, "Identification of dynamic loading on a bending plate using the virtual fields method," *Journal of Sound and Vibration*, vol. 333, pp. 7151–7164, 2014.

[2] C. Pezerat and J.-L. Guyader, "Two inverse methods for localization of external sources exciting a beam," *Acta Acustica*, vol. 3, pp. 1–10, 1995.

[3] A. N. Thite and D. J. Thompson, "The quantification of structure-borne transmission paths by inverse methods. part 2: Use of regularization techniques," *Journal of Sound and Vibration*, vol. 264, pp. 433–451, 2003.

[4] G. Chardon, L. Daudet, A. Peillot, F. Ollivier, N. Bertin, and R. Gribonval, "Near-field acoustic holography using sparse regularization and compressive sampling principles," *Journal of the Acoustical Society of America*, vol. 132, no. 3, pp. 1521–1534, 2012.

[5] M. Aucejo, "Structural source identification using a generalized tikhonov regularization," *Journal of Sound and Vibration*, vol. 333, pp. 5693–5707, 2014.

[6] A. Rezayat, V. Nassiri, B. D. Pauw, J. Ertveldt, S. Vanlanduit, and P. Guillaume, "Identification of dynamic forces using group-sparsity in frequency domain," *Mechanical Systems and Signal Processing*, vol. 70-71, pp. 756–768, 2016.

[7] E. Lourens, E. Reynders, G. D. Roeck, G. Degrande, and G. Lombaert, "An augmented kalman filer for force identification in structural dynamics," *Mechanical Systems and Signal Processing*, vol. 27, pp. 446–460, 2012.

[8] G. Enzner and P. Vary, "Frequency-domain adaptive kalman filter for acoustic echo control in hands-free telephones," *Signal Processing*, vol. 27, pp. 446–460, 2012.

[9] J. Ghibaudo, M. Aucejo, and O. D. Smet, "A sparse adaptive bayesian filter for input estimation problems," *Mechanical Systems and Signal Processing*, vol. 180, p. 109416, 2022.

[10] M. E. Tipping, "Sparse bayesian learning and the relevance vector machine," *Journal of Machine Learning Research*, vol. 1, pp. 241–244, 2001.

[11] D. Garcia, "Robust smoothing of gridded data in one and higher dimensions with missing values," *Computational Statistics & Data Analysis*, vol. 54, no. 4, pp. 1167–1178, 2010.